

# Nuclear Magnetic Resonance Investigations of Configurational Non-rigidity in Dinuclear Platinum(IV) Complexes. Part 8.<sup>1</sup> Fluxional Properties of Complexes

## $[(\text{PtXMe}_3)_2(\text{SCH}_2\text{SCH}_2\text{SCHMe})]$ (X = Cl, Br or I)

Edward W. Abel, David Ellis, Keith G. Orrell\* and Vladimir Šik

Department of Chemistry, University of Exeter, Exeter EX4 4QD, UK

A synthetic route to the platinum(IV) complexes  $[(\text{PtXMe}_3)_2(\text{SCH}_2\text{SCH}_2\text{SCHMe})]$  (X = Cl, Br or I) has been established. Solution NMR and other evidence favour the ligand adopting a boat conformation and bridging the two platinum(IV) centres across an  $-\text{SCH}_2\text{S}-$  portion of the ring, with the ring methyl group in an equatorial environment. Only very weak evidence was obtained for the existence of the  $-\text{SCHMeS}-$  bridged ligand complex despite the occurrence of a fluxional process involving  $60^\circ$  pivots of the ligand about individual S–Pt bonds which must proceed *via* the  $-\text{SCHMeS}-$  bridged species. Activation energies and a proposed mechanism for the process are presented. Some rare examples of  $^2J(\text{Pt}^{\text{IV}}\text{Pt}^{\text{IV}})$  scalar couplings are reported.

Trimethylplatinum(IV) halides form stable dinuclear complexes with open-chain and cyclic sulfur ligands which possess the moiety  $-\text{SCHZS}-$  (Z = H, Me or SMe). Examples of such complexes are  $[(\text{PtXMe}_3)_2\text{L}]$  where L =  $\text{MeSCH}_2\text{SMe}$ ,<sup>2</sup>  $\text{MeSCHMeSMe}$ ,<sup>2</sup>  $\text{MeSCH(SMe)SMe}$ ,<sup>1</sup>  $\text{SCH}_2\text{SCH}_2\text{SCH}_2$ ,<sup>3</sup> or  $\text{SCH}_2\text{SCH}_2\text{SCH}_2\text{SCH}_2$ .<sup>4</sup> These complexes display fascinating fluxionality which includes six-membered ring reversals, pyramidal sulfur inversions, ligand sulfur atom commutations and platinum–methyl scramblings. More specifically, the complexes of the cyclic ligands in 1,3,5-trithiane and 1,3,5,7-tetrathiocane exhibit novel platinum–sulfur shifts which equalise all ligand methylene environments. NMR observations of this process suggest a series of  $60^\circ$  or  $90^\circ$  pivots of the ligand about individual S–Pt bonds. However, no such process was detected for the complexes of the hindered ligand  $\beta$ -2,4,6-trimethyl-1,3,5-trithiane.<sup>3</sup> This ligand is thought to adopt the usual chair conformation of a six-membered ring in contrast to the boat conformation of 1,3,5-trithiane which is preferred on steric grounds when this ligand bridges two  $\text{PtXMe}_3$  moieties.

We have now synthesised the ligand  $\text{SCH}_2\text{SCH}_2\text{SCHMe}$  and isolated complexes  $[(\text{PtXMe}_3)_2(\text{SCH}_2\text{SCH}_2\text{SCHMe})]$  (X = Cl, Br or I). The aims of this paper are to investigate the conformation of this six-membered ring when acting as a bridging ligand, its mode of bridging two  $\text{PtXMe}_3$  moieties and, in particular, to examine whether any ligand 1,3 commutation occurs in this monomethyl derivative of 1,3,5-trithiane in contrast to its rigid 2,4,6-trimethyl derivative.

### Experimental

**Materials.**—All preparations were performed using standard Schlenk procedures. Elemental analyses were carried out by Butterworth Laboratories, Teddington, Middlesex. Melting points were recorded on a digital Gallenkamp apparatus and were uncorrected.

The ligand 2-methyl-1,3,5-trithiane<sup>5,6</sup> and trimethylplatinum(IV) halides  $[(\text{PtXMe}_3)_4]$ <sup>7–9</sup> were prepared by standard literature methods. All three complexes were prepared similarly. The procedure for the chloride complex  $[(\text{PtClMe}_3)_2(\text{SCH}_2\text{SCH}_2\text{SCHMe})]$  **1** is outlined below.

The complex  $[(\text{PtClMe}_3)_4]$  (0.11 g, 0.10 mmol, based on the

**Table 1** Characterisation data for the complexes  $[(\text{PtXMe}_3)_2(\text{SCH}_2\text{SCH}_2\text{SCHMe})]$

Complex	X	Yield (%) <sup>a</sup>	M.p./°C	Analysis (%) <sup>b</sup>	
				C	H
<b>1</b>	Cl	61	165	17.1	3.70
				(17.60)	(3.70)
<b>2</b>	Br	47	171	15.20	3.30
				(15.30)	(3.25)
<b>3</b>	I	52	182	<sup>c</sup>	<sup>c</sup>

<sup>a</sup> Yields quoted relative to the  $\text{PtXMe}_3$  unit. <sup>b</sup> Calculated values in parentheses. <sup>c</sup> Not available.

$\text{PtClMe}_3$  unit) and 2-methyl-1,3,5-trithiane (0.035 g, 0.23 mmol) were dissolved in warm benzene (10 cm<sup>3</sup>) and heated under reflux for 2 h. The clear solution was then concentrated to dryness *in vacuo* to give a white solid, and excess of ligand removed from the solid by sublimation *in vacuo*. Any unreacted  $[(\text{PtClMe}_3)_4]$  was removed by extracting the complex into cold acetone and filtering. Solvent was removed *in vacuo* and the residue recrystallised from hexane. Yield 0.86 g (61%). Characterisation data for the complexes are given in Table 1.

**NMR Spectra.**—Hydrogen-1 NMR spectra were recorded on a Bruker AM 250 FT spectrometer operating at 250.13 MHz. Spectra at ambient temperatures were obtained from  $\text{CDCl}_3$  solutions of the complexes. Dynamic spectra at above-ambient temperatures were based on  $\text{C}_6\text{D}_5\text{NO}_2$  solutions. Proton shifts are relative to  $\text{SiMe}_4$  as an internal standard. The  $^{195}\text{Pt}\{-^1\text{H}\}$  spectra were recorded on the above instrument at 53.53 MHz, shifts being quoted relative to the absolute scale  $\Xi(^{195}\text{Pt}) = 21.4$  MHz. A standard BVT-100 unit was used to control the magnet probe temperature. The calibration of this unit was checked regularly against a Comark digital thermometer. Rate data from  $^{195}\text{Pt}$  NMR spectra were based on bandshape analysis using the authors' version of the original DNMR3 program<sup>10</sup> and involved visual fittings of experimental and computer-simulated signals.

Platinum-195 two-dimensional exchange spectroscopy (EXSY) experiments were obtained with the Bruker automation program NOESYX incorporating the pulse sequence D1–90°–

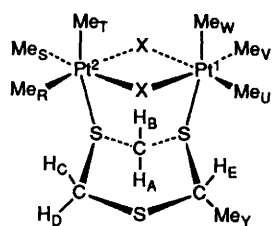


Fig. 1 Structure of the complexes  $[(PtXMe_3)_2(SCH_2SCH_2SCHMe)]$  ( $X = Cl, Br$  or  $I$ ) showing the Pt and H atom labelling

D0–90°–D9–90°–FID (free induction decay). The relaxation delay D1 was 2 s and D0 had an initial value of  $3 \times 10^{-10}$  s. The mixing time D9 ( $\tau_m$ ) was chosen from within the range 0.1–0.5 s. Optimum values are given later. The frequency domain F1 contained 256 words, zero-filled to 512 words and the dimension F2 contained 512 words. No random variation of D9 ( $\tau_m$ ) was provided since no scalar couplings were present. The spectral width was typically set at 1400 Hz and the number of pulses per experiment was 128. The data were processed using an unshifted sine-bell window function in both dimensions. Magnitude-mode spectra were calculated with symmetrisation about the diagonal. Rate data were extracted from the two-dimensional EXSY contour plots using our D2DNMR program described previously.<sup>11–13</sup>

## Results and Discussion

**Preparation and Structure of the Complexes.**—The three complexes  $[(PtXMe_3)_2(SCH_2SCH_2SCHMe)]$  ( $X = Cl, Br$  or  $I$ ) were obtained in moderate yields by refluxing benzene solutions of the ligand with the appropriate trimethylplatinum(IV) halide (Table 1). Solution NMR spectra in the temperature range –10 to 10 °C supported the static dinuclear structures in Fig. 1, where the ligand adopts a boat conformation and bridges the platinum centres *via* an –SCH<sub>2</sub>S– as opposed to a –SCHMeS– unit.

**<sup>1</sup>H NMR Studies.**—*Static spectra.* Solutions of the complexes in CDCl<sub>3</sub> when cooled somewhat below room temperature gave well resolved NMR signals. The spectra of  $[(PtClMe_3)_2(SCH_2SCH_2SCHMe)]$  at 10 °C are shown in Fig. 2 and are illustrative of all three complexes. Chemical shift and scalar coupling constant data are contained in Tables 2 and 3.

The ring methylene region resolves essentially into two AB quartets plus a binomial intensity quartet. The AB quartet of the methylene group bridging the two co-ordinated S atoms is centred at higher frequency due to the combined co-ordinative deshielding effects of the two Pt nuclei. Hydrogen H<sub>A</sub> is assigned a pseudo-axial position on the basis of its large  $^3J(PtH)$  coupling to  $^{195}Pt^2$  arising from the near 180° dihedral angle<sup>14,15</sup> relating the Pt–S–C and S–C–H planes (Fig. 1). Similarly, H<sub>C</sub> is assigned a pseudo-axial position on the basis of an observable  $^{195}Pt$  satellite. Hydrogens H<sub>B</sub> and H<sub>D</sub> exhibit no coupling to  $^{195}Pt$  due to near 109° dihedral angles associated with pseudo-equatorial positions. The methine hydrogen H<sub>E</sub> (Fig. 1) appears as a binomial quartet (due to three-bond coupling to the geminal methyl group) which overlaps the H<sub>C</sub> signals. It is assigned a pseudo-axial position as it is highly probable on steric grounds that the ring methyl will adopt a pseudo-equatorial position. Such an orientation would be confirmed by measurable scalar coupling of H<sub>E</sub> to  $^{195}Pt^1$ . Unfortunately, the multiplet nature of the H<sub>E</sub> signal rather masks the  $^{195}Pt$  satellite signals, although a hint of such signals appears to the high-frequency side of the multiplet [Fig. 2(a)]. The general pattern of  $^3J(PtH)$  couplings (Table 3) strongly supports a boat conformation for the 2-methyl-1,3,5-trithiane ring. The arguments have been laid out previously for the unsubstituted cyclic ligand complexes.<sup>3</sup>

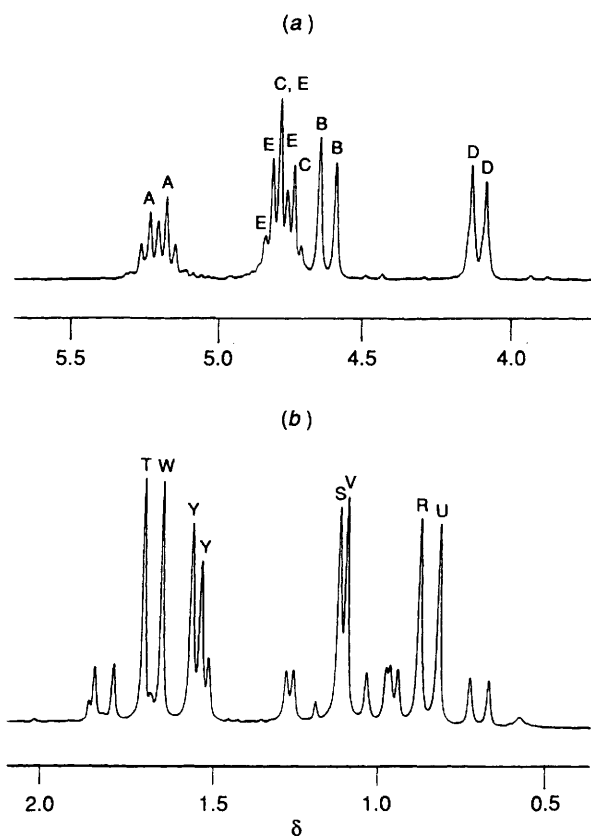


Fig. 2 Proton NMR spectrum (250 MHz) of  $[(PtClMe_3)_2(SCH_2SCH_2SCHMe)]$  at 10 °C in CDCl<sub>3</sub>: (a) the ring proton and (b) the methyl region

The methyl regions of the  $^1H$  spectra of the three complexes are easily analysed and that for  $[(PtClMe_3)_2(SCH_2SCH_2SCHMe)]$  is shown in Fig. 2(b). Signals due to the six non-equivalent Pt–Me environments are seen, each with its accompanying pair of  $^{195}Pt$  satellites due to  $^2J(PtH)$  coupling. Assignments in the first instance are based on the well established observation in halide-bridged dinuclear platinum(IV) complexes<sup>1–4</sup> that equatorial Pt–Me (*trans* to X) resonate to lower frequencies of axial Pt–Me (*trans* to S), and have somewhat larger  $^2J(PtH)$  coupling constants reflecting the different *trans* influences of halide and sulfur. The two Pt–Me groups R and U which are closest to the ligand methylene and methine protons are assigned to the lowest-frequency signals in accordance with previous arguments.<sup>3,16</sup> The other methyl pair S and V, being more remote from the ring methyl group, will be less affected by the asymmetry of the ligand ring. The full assignments shown in Fig. 2 and Table 3 are not totally certain and for each pair of signals [labelled R/U, S/V and T/W, Fig. 2(b)] assignments might possibly be reversed. This region of the spectrum also depicts the 1:1 doublet of the ring methyl group Y.

Thus, all major signals in the spectra can be accounted for in terms of the complex illustrated in Fig. 1, where the trithiane ligand bridges the two platinum centres by an –SCH<sub>2</sub>S– section of the ring. A structure containing a bridging –SCHMeS– moiety would possess a symmetry plane bisecting the Pt...Pt vector, and would give rise to only one methylene AB quartet and two Pt–Me signals in its  $^1H$  NMR spectrum. Careful examination of the methylene and methyl regions of the spectra did reveal some very weak additional signals. For instance, for complex 1 a weak AB quartet with chemical shifts of  $\delta$  3.91 and 4.46 is just visible in Fig. 2(a). There is, therefore, some supporting evidence for a very low percentage (*ca.* 1–2%) of the other co-ordination complex.

**Table 2** Static  $^1\text{H}$  NMR parameters\* for complexes  $[(\text{PtXMe}_3)_2(\text{SCH}_2\text{SCH}_2\text{SCHMe})]$  (methylene region)

Complex	X	$T/^\circ\text{C}$	$\delta$					$J(\text{H}_\text{A}\text{H}_\text{B})$	$J(\text{H}_\text{C}\text{H}_\text{D})$	$J(\text{H}_\text{E}\text{H}_\text{F})$
			$\text{H}_\text{A}$	$\text{H}_\text{B}$	$\text{H}_\text{C}$	$\text{H}_\text{D}$	$\text{H}_\text{E}$			
1	Cl	10	5.21 (14.48)	4.63	4.77 (12.11)	4.12	4.81	15.66	12.50	7.17
2	Br	10	5.49 (15.25)	4.80	4.88 (13.17)	4.11	4.89	14.44	12.06	6.18
3	I	-10	5.94 (14.76)	5.03	5.22 (12.96)	4.23	5.18	14.02	12.57	6.95

\*  $J$  Values in Hz.  $^3J(\text{PtH})$  in parentheses.**Table 3** Static  $^1\text{H}$  NMR parameters for complexes  $[(\text{PtXMe}_3)_2(\text{SCH}_2\text{SCH}_2\text{SCHMe})]$  (methyl region)

Complex	X	$T/^\circ\text{C}$	$\delta$						
			$\text{Me}_\text{R}$	$\text{Me}_\text{S}$	$\text{Me}_\text{T}$	$\text{Me}_\text{U}$	$\text{Me}_\text{V}$	$\text{Me}_\text{W}$	$\text{Me}_\text{Y}$
1	Cl	10	0.88 77.5 <sup>a</sup>	1.12 77.4 <sup>a</sup>	1.70 71.8 <sup>a</sup>	0.83 77.2 <sup>a</sup>	1.10 76.5 <sup>a</sup>	1.65 69.4 <sup>a</sup>	1.54 7.17 <sup>b</sup>
2	Br	10	0.94 77.5 <sup>a</sup>	1.17 78.2 <sup>a</sup>	1.83 70.8 <sup>a</sup>	0.88 77.5 <sup>a</sup>	1.15 76.4 <sup>a</sup>	1.77 71.9 <sup>a</sup>	1.53 6.18 <sup>b</sup>
3	I	-10	1.13 74.3 <sup>a</sup>	1.38 74.4 <sup>a</sup>	2.11 73.5 <sup>a</sup>	1.06 74.0 <sup>a</sup>	1.35 74.6 <sup>a</sup>	2.05 72.9 <sup>a</sup>	1.69 6.95 <sup>b</sup>

<sup>a</sup>  $^2J(\text{PtH})/\text{Hz}$ . <sup>b</sup>  $^3J(\text{HH})/\text{Hz}$ .**Table 4** Static  $^{195}\text{Pt}$  NMR parameters for complexes  $[(\text{PtXMe}_3)_2(\text{SCH}_2\text{SCH}_2\text{SCHMe})]$ 

Complex	X	$T/^\circ\text{C}$	$\delta(\text{Pt}^1)^*$	$\delta(\text{Pt}^2)^*$	$^2J(\text{PtPt})/\text{Hz}$
1	Cl	0	1993.0	2008.4	$\approx 0$
2	Br	-20	1794.7	1809.2	7.5
3	I	-10	1367.2	1377.4	13.4

\* Relative to  $\Xi(^{195}\text{Pt}) = 21.4$  MHz.**Table 5** Rates of 1,3-ligand commutations in  $[(\text{PtXMe}_3)_2(\text{SCH}_2\text{SCH}_2\text{SCHMe})]$  complexes

$T/^\circ\text{C}$	Method <sup>a</sup>	Rate constants <sup>b/s</sup> <sup>-1</sup>		
		X = Cl	X = Br	X = I
-10	EXSY	—	—	0.70 (0.35)
0	EXSY	0.54 (0.3)	0.47 (0.3)	2.30 (0.25)
10	EXSY	1.38 (0.2)	1.66 (0.2)	8.1 (0.13), 5.0 <sup>c</sup>
20	EXSY	4.7 (0.13)	4.4 (0.13)	—
30	BSA	—	—	70
35	BSA	—	—	128
40	BSA	22	41	200
45	BSA	40	60	—
50	BSA	70	110	—
55	BSA	130	160	—
60	BSA	210	—	—

<sup>a</sup> EXSY = Two-dimensional exchange spectroscopy, BSA = one-dimensional bandshape analysis. <sup>b</sup> Mixing times,  $\tau_\text{m}/\text{s}$  in parentheses. <sup>c</sup> BSA value.

**Dynamic spectra.** When the sample temperature was raised by about  $15^\circ\text{C}$  gross changes occurred in both regions of the spectra of complexes 1–3, these changes being fully reversible on cooling. In the ring methylene region signals due to hydrogens  $\text{H}_\text{A}$  and  $\text{H}_\text{D}$  exchanged as did signals  $\text{H}_\text{B}$  and  $\text{H}_\text{C}$ . At sufficiently high temperatures these groups of signals coalesced and then sharpened towards a single averaged AB-type quartet. The methine signal of the  $-\text{CHMe}$  moiety remained unaffected by temperature. In the Pt–Me region the signals due to the four equatorial methyls coalesced to a broad singlet at *ca.*  $50^\circ\text{C}$ . Concurrently, the two axial methyl signals also coalesced. Further elevation of sample temperature led to a coalescence of

the axial and equatorial methyl signals to give a single signal which, when sufficiently sharp, exhibited  $^{195}\text{Pt}$  satellites.

These changes are all analogous to those observed in the spectra of the unsubstituted trithiane complexes<sup>3</sup> and may be similarly explained, namely by a series of 1,3 shifts of the cyclic ligand which cause all three S atoms to share co-ordination to the two platinum atoms at higher temperatures. This process subsequently induces a scrambling of the three Pt–Me environments so that axial and equatorial methyl groups become indistinguishable on the  $^1\text{H}$  NMR time-scale.

**$^{195}\text{Pt}$  NMR Studies.**—The fluxional process described above, namely commutation of the sulfur co-ordination sites, will lead to an exchange of the two platinum environments. It was therefore decided to follow the kinetics of this process by  $^{195}\text{Pt}$  NMR spectroscopy. Two sharp signals are observed at below-ambient temperatures, the lower-frequency signal being assigned to  $\text{Pt}^1$  by virtue of the slight shielding effect of the ring methyl group (Table 4). For complexes 2 and 3 both platinum signals exhibit partially resolved splittings which are interpreted as being due to two-bond Pt–Pt couplings and are thought to be the first reported examples of  $\text{Pt}^{\text{IV}}-\text{X}-\text{Pt}^{\text{IV}}$  couplings. Magnitudes of  $^2J(\text{PtPt})$  couplings *via* halide bridge atoms depend very strongly on the oxidation state of the platinum atoms and range from 125 to 390 Hz for  $\text{Pt}^{\text{II}}$  to immeasurably small values for most platinum(IV) complexes, *e.g.*  $[(\text{PtXMe}_3)_4]^{17}$  and  $[(\text{PtXMe}_3)_2(\text{L}-\text{L}')]$  ( $\text{L}-\text{L}' =$  bridging mixed chalcogen ligands).<sup>18</sup> The values given here for complexes 2 and 3 (Table 4) are very small in view of the relative closeness of the two coupling centres and increase slightly with increasing mass/size of the halogen. The chemical shifts are notably halogen dependent, exhibiting the well established trend to lower resonant frequencies as the atomic number of the halogen increases.<sup>19</sup> Temperature dependences of the shifts were also very significant with  $\delta$  values increasing with increasing sample temperature.

On warming  $\text{CDCl}_3$  solutions of the complexes to *ca.*  $60^\circ\text{C}$  both  $^{195}\text{Pt}$  NMR signals exhibited exchange broadening. Bandshape analysis of this two site-exchange process was carried out in the usual way in the temperature range  $30$ – $60^\circ\text{C}$ , and 'best-fit' rate constants for temperatures at  $5^\circ\text{C}$  intervals were calculated (Table 5).

In order to study this ligand commutation process over a wide range of temperatures, the two-dimensional EXSY

**Table 6** Activation parameters for 1,3-ligand commutations in complexes [(PtXMe<sub>3</sub>)<sub>2</sub>L]

X	L	E <sub>a</sub> /kJ mol <sup>-1</sup>	log <sub>10</sub> (A/s <sup>-1</sup> )	ΔH <sup>‡</sup> /kJ mol <sup>-1</sup>	ΔS <sup>‡</sup> /J K <sup>-1</sup> mol <sup>-1</sup>	ΔG <sup>‡a</sup> /kJ mol <sup>-1</sup>	Notes
Cl		71.6 ± 6.8	13.4 ± 1.3	69.2 ± 6.8	4 ± 24	68.1 ± 0.4	b, c
		98.7 ± 1.6	17.8 ± 0.3	96.0 ± 1.6	87 ± 5	70.1 ± 0.1	d, e
Cl		62.6 ± 1.2	13.5 ± 0.2	60.3 ± 1.2	6 ± 4	58.6 ± 0.1	f
Br		74.8 ± 3.9	14.0 ± 0.7	72.4 ± 3.9	15 ± 14	68.0 ± 0.2	b, c
		84.5 ± 3.2	15.7 ± 0.5	81.9 ± 3.2	46 ± 10	68.0 ± 0.2	d, g
Br		61.8 ± 1.5	13.3 ± 0.3	59.5 ± 1.5	2 ± 5	58.8 ± 0.2	f
I		75.6 ± 2.8	14.9 ± 0.5	75.5 ± 2.8	32 ± 10	63.9 ± 0.3	b, h
		82.9 ± 6.4	16.1 ± 1.1	80.3 ± 6.4	55 ± 21	63.8 ± 0.2	d, i

<sup>a</sup> Values at 298.15 K. <sup>b</sup> <sup>195</sup>Pt EXSY derived values. <sup>c</sup> Based on range 0–20 °C. <sup>d</sup> <sup>195</sup>Pt BSA derived values. <sup>e</sup> Range 40–60 °C. <sup>f</sup> <sup>1</sup>H BSA values (ref. 3). <sup>g</sup> Range 30–55 °C. <sup>h</sup> Range –10 to 10 °C. <sup>i</sup> Range 30–40 °C.

method<sup>13,20</sup> was applied. This involved accurate volume integration of the four signals (diagonal + cross-peaks) in the EXSY contour plots and inputting these data into the D2DNMR program.<sup>11</sup> The calculated 2 × 2 kinetic matrix contains the required rate constants as off-diagonal terms. The accuracy of these values is very dependent on the mixing time used in the radiofrequency pulse sequence. Optimum values were chosen by experiment and the resultant rate data are contained in Table 5.

**Evaluation of Energy Barriers.**—Two distinct dynamic processes have been shown to operate in these complexes, namely a 1,3 commutation of the ligand co-ordination sites and an exchange or scrambling of the Pt–Me environments. Platinum-195 NMR spectra are sensitive only to the ligand movement whereas <sup>1</sup>H spectra are sensitive to both processes. In our previous studies of the unsubstituted trithiane<sup>3</sup> and tetrathiocane<sup>4</sup> complexes emphasis was placed on the dynamic <sup>1</sup>H NMR spectra for measuring activation energies of both processes. In this paper we concentrate on the role of <sup>195</sup>Pt NMR spectra in probing the ligand dynamics. Energy data based on both one- and two-dimensional <sup>195</sup>Pt spectra were calculated and show remarkably good agreement (Table 6). A very slight discrepancy in the two data sets for the chloride complex **I** may be due to the onset of a ligand dissociation/association process occurring in the somewhat higher temperature range over which bandshape analysis had to be performed. Such a bond breaking/remaking process is perhaps implied by the sizeable entropy of activation in this case.

The energies of the ligand commutation process as expressed by ΔG<sup>‡</sup> values (at 298.15 K) are significant in that they are approximately 10 kJ mol<sup>-1</sup> higher than for the unsubstituted 1,3,5-trithiane complex<sup>3</sup> and appear to be somewhat halogen dependent with values decreasing with increasing halogen mass/size, particularly on changing from bromine to iodine. In the absence of similar data for [(PtIme<sub>3</sub>)<sub>2</sub>(SCH<sub>2</sub>SCH<sub>2</sub>SCH<sub>2</sub>)]<sup>3</sup> it is not clear whether a similar trend exists for the unsubstituted 1,3,5-trithiane complexes, but it would seem very likely.

**Proposed Mechanism of the Ligand 1,3 Commutation.**—In our previous study of the 1,3,5-trithiane complexes,<sup>3</sup> it was shown that the mechanism which fully accounts for the NMR changes in both the ligand methylene and Pt–Me regions of the <sup>1</sup>H NMR spectrum was one involving a series of pivots through angles of 60° about either S–Pt bond. Such a process interchanges co-ordinated and unco-ordinated S atom pairs, and in the process averages ring methylene environments and the four equatorial Pt–Me environments. In the present complexes a single 60° S–Pt pivot converts the favoured ground-state structure into the less favoured –SCHMeS– bridged structure. There are, therefore, two ground-state structures, the –SCH<sub>2</sub>S– bridged or boat form **I** and the –SCHMeS– bridged or boat form **II**, between which the fluxional process occurs. This is in contrast to the single –SCH<sub>2</sub>S– bridged ground-state

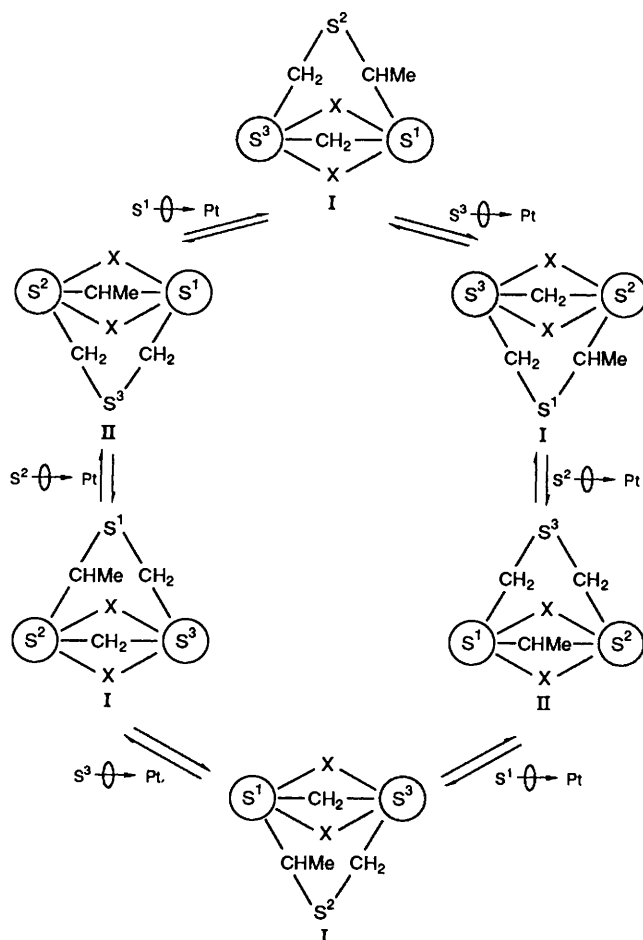


**Fig. 3** The pivot mechanism for ligand 1,3 commutation in the complexes [(PtXMe<sub>3</sub>)<sub>2</sub>(SCH<sub>2</sub>SCH<sub>2</sub>SCHMe)]. Circled S atoms denote Pt-bonded sulfurs. Pivots about S<sup>1</sup>–Pt or S<sup>2</sup>–Pt bonds cause boat form **I** ⇌ **II** exchanges whereas S<sup>3</sup>–Pt pivots exchange enantiomeric **I** forms

structure in the unsubstituted trithiane complexes.<sup>3</sup> There are, therefore, now two theoretically distinct exchange pathways for the ligand commutation, namely boat form **I** ⇌ **I** or **I** ⇌ **II** exchanges. However, since the –SCHMeS– bridged complex **II** does not contribute significantly to the observable spectrum only one type of pathway is actually detectable by NMR spectroscopy. The full mechanism is illustrated in Fig. 3 where 60° pivots about S<sup>1</sup>–Pt, S<sup>2</sup>–Pt or S<sup>3</sup>–Pt bonds may occur. The S<sup>3</sup>–Pt pivots lead to boat form **I** ⇌ **I** exchange and are therefore directly NMR detectable. Individual pivots about S<sup>1</sup>–Pt are undetectable since the boat form **II** species are present in solution to only a vanishingly low extent. However, consecutive S<sup>1</sup>–Pt/S<sup>2</sup>–Pt pivots are equivalent to single pivots

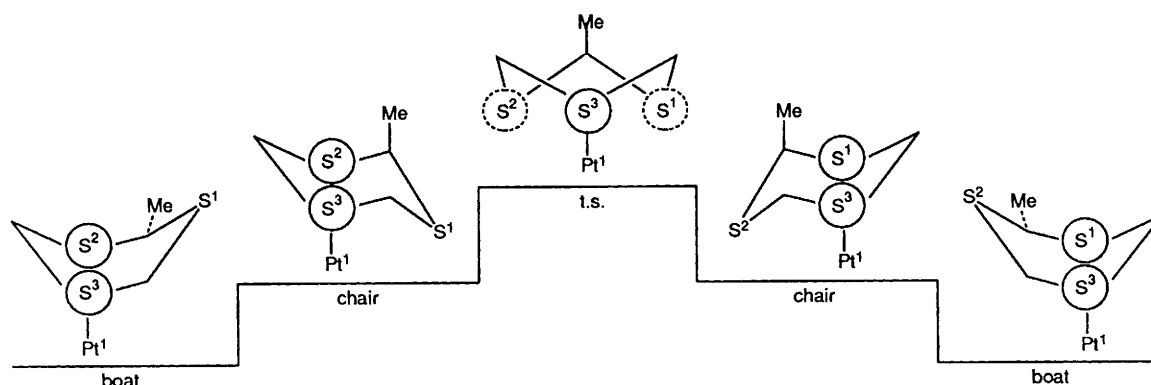


Fig. 4 The proposed pathway for a  $60^\circ$  pivot about a  $S^3$ -Pt bond showing the intermediate chair forms and the transition-state (t.s.) structure. Circled S atoms denote co-ordinated sulfurs. In the t.s. structure the broken circles imply shared co-ordination to the  $Pt^2$  atom

about the  $S^3$ -Pt bond and therefore the activation energies quoted above can relate to either of these cases.

Any one of these  $60^\circ$  pivots is thought to proceed *via* the two chair forms of the corresponding boat conformer. For example, the case of a pivot about the  $S^3$ -Pt<sup>1</sup> bond is illustrated in Fig. 4. The boat structure I is first converted into the chair structure so that the unco-ordinated  $S^1$  atom is in place to receive the  $Pt^2$  atom when it swings into place. The resulting structure is the enantiomer of the chair form which then reverts to its energetically more favoured boat form which is the enantiomer of the starting boat structure I. Fig. 4 depicts the two chair intermediates and the transition-state structure (t.s.). In the latter structure  $S^3$  is strongly bonded to  $Pt^1$  and both  $S^1$  and  $S^2$  are weakly bonded to  $Pt^2$ . Similar diagrams can be drawn for pivots about the  $S^1$ -Pt and  $S^2$ -Pt bonds, the difference now being that the resulting boat structures and intermediate chair structures are no longer degenerate and will possess different ground-state energies.

We propose such a scheme as the most reasonable rationalisation of the ligand fluxionality in these 2-methyl-1,3,5-trithiane complexes. It is unfortunate that the virtual absence of the -SCHMeS- bridged complex precludes direct evidence of all six stages of the pivot mechanism (Fig. 3).

## References

1 Part 7, E. W. Abel, T. E. MacKenzie, K. G. Orrell and V. Šik, *J. Chem. Soc., Dalton Trans.*, 1986, 2173.

- 2 E. W. Abel, A. R. Khan, K. Kite, K. G. Orrell and V. Šik, *J. Chem. Soc., Dalton Trans.*, 1980, 2208.
- 3 E. W. Abel, M. Booth, G. King, K. G. Orrell, G. M. Pring and V. Šik, *J. Chem. Soc., Dalton Trans.*, 1981, 1846.
- 4 E. W. Abel, G. D. King, K. G. Orrell, V. Šik, T. S. Cameron and K. Jochem, *J. Chem. Soc., Dalton Trans.*, 1984, 2047.
- 5 D. Seebach and A. K. Beck, *Org. Synth.*, 1971, **51**, 39.
- 6 D. Seebach, E. J. Corey and A. K. Beck, *Chem. Ber.*, 1974, **107**, 367.
- 7 J. C. Baldwin and W. C. Kaska, *Inorg. Chem.*, 1975, **14**, 2020.
- 8 D. E. Clegg and J. R. Hall, *J. Organomet. Chem.*, 1970, **22**, 491.
- 9 D. H. Goldsworthy, Ph.D. Thesis, University of Exeter, 1980.
- 10 D. A. Kleier and G. Binsch, DNMR3 Program 165, Quantum Chemistry Program Exchange, Indiana University, 1970.
- 11 E. W. Abel, T. P. J. Coston, K. G. Orrell, V. Šik and D. Stephenson, *J. Magn. Reson.*, 1986, **74**, 34.
- 12 E. W. Abel, I. Moss, K. G. Orrell, V. Šik and D. Stephenson, *J. Chem. Soc., Dalton Trans.*, 1987, 2695.
- 13 E. W. Abel, V. Šik and D. Stephenson, *Prog. Nucl. Magn. Reson. Spectrosc.*, 1990, **22**, 141.
- 14 M. Karplus, *J. Chem. Phys.*, 1959, **30**, 11.
- 15 M. Karplus, *J. Am. Chem. Soc.*, 1963, **85**, 2870.
- 16 E. W. Abel, A. R. Khan, K. Kite, K. G. Orrell and V. Šik, *J. Chem. Soc., Dalton Trans.*, 1980, 2220.
- 17 T. G. Appleton and J. R. Hall, *Aust. J. Chem.*, 1980, **33**, 2387.
- 18 E. W. Abel, K. G. Orrell and V. Šik, unpublished work.
- 19 P. S. Pregosin, *Annu. Rep. N.M.R. Spectrosc.*, 1986, **17**, 285.
- 20 R. Willem, *Prog. Nucl. Magn. Reson. Spectrosc.*, 1987, **20**, 1.

Received 15th July 1992; Paper 2/03758K